Development of an Optimized Hybrid Magnetometer for Earth's Magnetic Field Studies

Okunola, I. O[1]. Agbi J. I[2] Effiong, E.E[3] & Oluborode, G.B[4]
[1,3]National Centre for Energy and Environment (Energy Commission of Nigeria),
University of Benin, Benin City.
[2]Department of Physics and Electronics, Adekunle Ajasin University,
Akungba Akoko, Ondo State
[4]National Institute for Freshwater Fisheries Research,
P. M. B. 6006, New Bussa, Niger State
Corresponding author: okunolaisraeloo@gmail.com, +2348061379083
DOI: 10.56201/rjpst.vol.8.no4.2025.pg9.26

Abstract
The design of hybrid magnetometers is typically a nonlinear multi-objective optimization problem. Sometimes, an optimal magnetometer performance is difficult to achieve due to low sensitivity sensors which decrease with an increase in noise level while trying to reduce the sensor dimension. Moreover, these approaches are too difficult, slow, time consuming, expensive, and do not produce optimal magnetometer performance. As a result, little attempt has been made to develop hybrid magnetometer sensor. Thus far, no existing magnetometer device has incorporated two sensors, combined in a single unit device that can measure earth's magnetic fields in three co-ordinates direction simultaneously. This observed situation prompted the development of a locally made hybrid magnetometer device that can determine magnetic field in 3-dimensional X, Y and Z coordinates variation of the earth and total magnetic field. The developed magnetometer device consisted HMC5883 and proton precession sensors combined in a single unit that determined magnetic field of X, Y and Z axis simultaneously. The data logger was wired and hand-assembled utilizing a factory-built-in HMC5883 and Proton Procession sensors combined with Arduino Uno328 micro-controller, which contains ADC, real time clock, data storage, voltage regulator (ICLM7805) and kerosene. The device detects the X, Y and Z co-ordinates of the magnetic field in analog form. The data were digitized using analog-to-digital-converter (ADC) which were processed by micro-controller and later displayed through liquid crystal display (LCD) screen. The data were also automatically saved in an SD card in Excel format. The measurements variations of the earth residual magnetic field were taken spatially, giving a minimum value of 363.1172nT for the magneto resistive magnetometer, 357.205nT for proton precession magnetometer and 361.708nT for the geometric smart magnetometer; and giving a maximum value of 366.6396nT for the magneto resistive magnetometer, 360.683nT for proton precession magnetometer and 365.792nT for the geometric smart magnetometer. The locally developed hybrid magnetometer is cheaper and with sufficient accuracy compared with the imported equipment which is more expensive and with low accuracy. It is recommended that the equipment be used by geophysical researchers

Keywords: *Micro-controller, magnetometer, magnetic field, magneto-resistive sensor, geometric smart magnetometer.*

1. INTRODUCTION

Magneto-resistive effect is used for determining the presence of a magnetic field, their strength and the direction of the force. It is made up of the indium antimonide or indium arsenide semiconductor material. The an-isotropic magneto-resistive (AMR) effect was first described in 1857 by William Thomson (Thomson, 2004). Thomson observed that the resistivity of ferromagnetic materials depends on the angle between the direction of electric current and the orientation of magnetization.

The first technical applications of this effect were introduced 100 years later, when the theoretical and practical prerequisites for the realization of thin film AMR sensors were obtained. In the following years, AMR sensors were primarily used as read heads in magnetic hard disk drives. Thanks to their simplicity of design, low cost, robustness and temperature stability, they were introduced in a wide range of industrial applications, including automotive, consumer electronics or biotechnology. In automotive and consumer electronic applications, magneto-resistive (MR) sensors are used for current sensing or position, speed and angle sensing as well as Earth's magnetic field sensing in compass applications. In biotechnology, MR sensors are used for bi-molecular detection in protein assays using magnetic tags or in micro fluidic systems for magnetic bead manipulation. (David et al., 2013).

The earth's magnetic field intensity is about 0.0005 to 0.0006 nano Tesla and has a component parallel to the earth's surface that always point toward magnetic north (Campbell, 2015). The basis for magnetic compasses. The balanced needle compass is only a slight variation of this early discovery. But advancement in technology has to the solid-state electronic compass based on MR magnetic sensors and acceleration-based tilt sensors. Electronic compasses offer many advantages over conventional needle type or gimbaled compasses such as: shock and vibration resistance, electronic compensation for stray field effects, and direct interface to electronic navigation systems. (Korepanov and Marusenkov, 2017).

In this work, three navigational references have been used: the X component will be in the forward-looking direction, the Y component to the right, and the Z component will be down. This is in confirmation of (Matsuoka et al,. 2017) postulate that there are X, Y and Z coordinates for navigational reference. This research aimed at developing a locally made 3- Dimensional optimized magneto-resistive magnetometer from high precession sensor capable of logging magnitude and direction.

In order to achieve the proposed aim of the research, the following specific objectives were generated:

- Development of low cost 2 in 1 magnetometer.
- Compare the performance of the locally developed magneto-resistive magnetometer with imported magnetometer.
- to monitor the changes in Earth's magnetic field using high precision sensors such as HMC5883 and Hydrocarbon Sensor.

The calibrations of locally made equipment with imported Geometric Smart Magnetometer (GSM-19T) were carried out along Library and Senate Building Road at Adekunle Ajasin University campus, Akungba Akoko. Ondo State.

Magnetometers Measurement Applications

There is a growing concern among the researchers and practitioners on the subject matter of magnetometer. The reason may be that magnetometer is often seen as one of the scientist's tools in the scientist's world due to its substantial cost and its usefulness (Grosz and Paperno, 2012).

Scholars have also submitted that magnetometer is an instrument that measures magnetism either the magnetization of a magnetic material like a Ferro magnet, or the direction, strength, or relative change of a magnetic field at a particular location. Thus, a compass is a simple type of magnetometer, one that measures the direction of an ambient magnetic field. One of the first magnetometer capable the absolute magnetic intensity measurement was invented by Carl Friedrich Gauss in 1833 and notable developments in the 19th century included the Hall Effect, which is still widely used (Grosz and Paperno, 2012).

The magneto-resistive sensor utilized in the single-axis magnetometer is a HMC1001 microcircuit device from Honeywell Inc. The magneto-resistor is composed of a Ni–Fe Permalloy patterned element deposited on Si wafer and the sensor is comprised of four such magneto-resistors implemented as a Wheatstone bridge. Each component resistor has been magnetized along its easy (long) axis during manufacture, and the hard (short) axis corresponds to the field sensitive direction. The magnetization directions of each half bridge element are opposite to each other and this doubles the bridge output compared with that of the single sensor as well as providing for improved temperature stability (Gordon and Brown 2015).

2. METHODOLOGY

Design and Development of Hybrid Magnetometer System

Design and construction of hybrid magnetometer system was developed in two main subsystems as follows:

1. data collection subsystem, which consists of HMC5883L and Proton Precession Sensors with ADC converter. The sensor sends values to the micro-controller that collects the data, process, analyze and present it on the LCD and the simultaneously record them in the SD card.
2. data management subsystem, which accesses the data and displays the same to the end user.

   The following components were used to develop hybrid magnetometer with magneto-resistive and proton precession sensors. HMC5883 Sensors with three axis co-ordinates (figure 2), Analog-to-digital converters, Arduino Uno328 Microcontroller, LM2596 Voltage regulator, PPM coil sensor, RTC module, Liquid Crystal Display (LCD), Micro SD card module, resistors and kerosene.

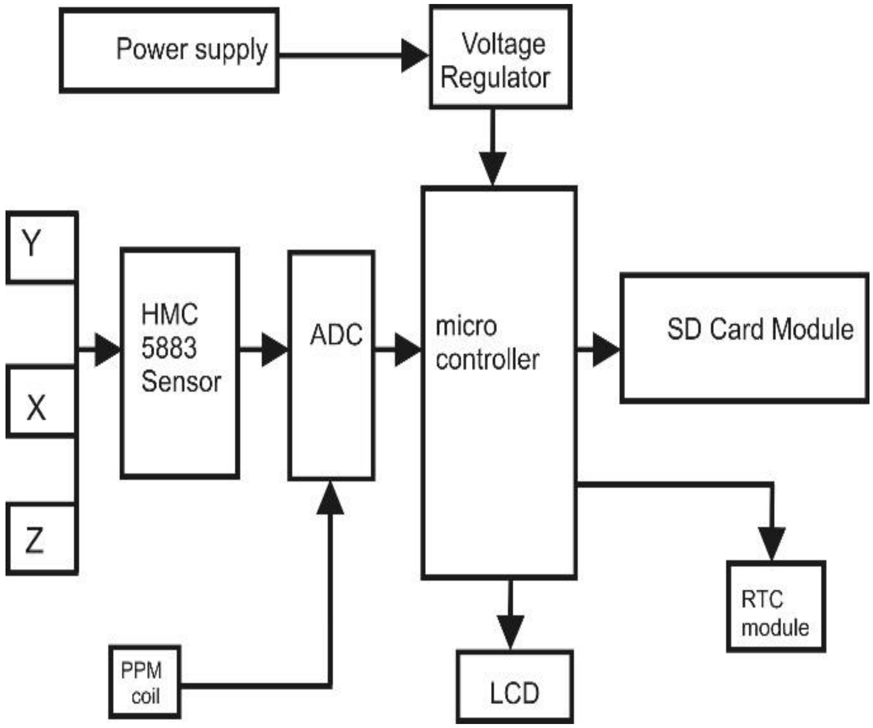

Figure 1: Block Diagram of Magnetometer with 3-axis HMC5883 and PPM Sensors.

All these components were connected together (see Figure 1) with appropriate embedded program using micro-controller platform for decoding signal and displayed data. The magnetic field in X, Y and Z axis were automatically detected under the control of single chip micro-controller. Both units are connected to measure the magnetic field of a location using two different sensors and display their values consecutively on the LCD screen and the same time store the logged data in an SD card attached to the device. The heart of the device is Atmega328 Arduino uno, which is programmed on a C++ platform. This micro-controller supervises the reading of the two sensors attached to it, process the analog values from them, calibrate and display them as appropriate. Arduino is interfaced to the 16 x 4 LCD display using the parallel connection method on pin (13, 12, 5, 4, 3, 2) as (RS, EN, D_4, D_5, D_6, D_7) respectively.
The HMC5883L is the magneto-resistive magnetometer sensor connected in I^2C format (SDA, SCL) (A5, A4) to the micro-controller.

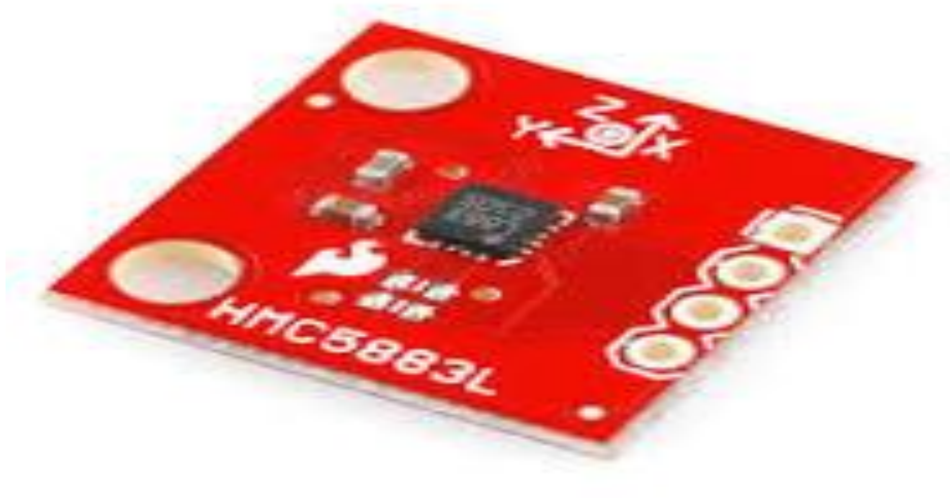

Figure 2: An X, Y and Z (HMC5883) Sensor (Coillot and Moutoussamy, 2013)

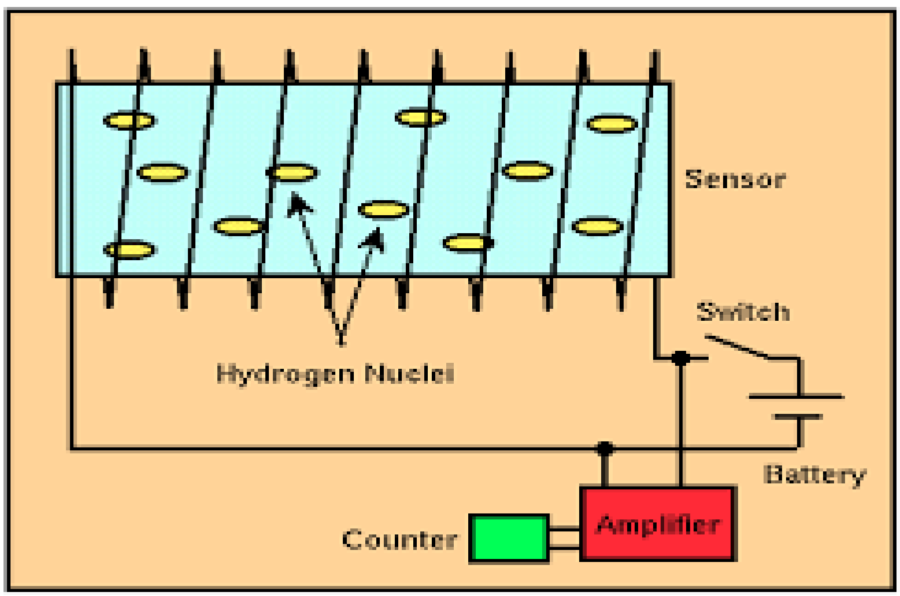

Figure 3: A Bottle Containing Hydrocarbon (Kerosene) and Winding Coil

The Proton precession magnetometer sensor is made by winding 200turns of SWG 20 wire coil round a dark short bottle filled with kerosene, this coil is exited with a 12v DC power source pick up coil that becomes charged because of the hydrogen ion generated by the kerosene, this makes the sensor sensitive to pick magnetic field to be measured. It is connected to the analog pin AD0 of the micro-controller. The SD card is attached to Arduino microcontroller using the Serial Peripheral interface (SPI) format Master Out Slave in (MOSI), Master in Slave Out (MISO), Serial Clock (SCK) and Computer System (CS) pin of the SD card are connected to the Arduino pin 13, 12, 11 and 10. Plastic bottle is used as container being non-magnetic and do not alter the local geomagnetic field. Kerosene is preferred as the proton rich sample; kerosene was used due to its low cost and ease of use.

The whole unit is powered from a 7.2V, 3.8A lithium battery. The battery can be recharged by using an electric cord connected to power supply mains.

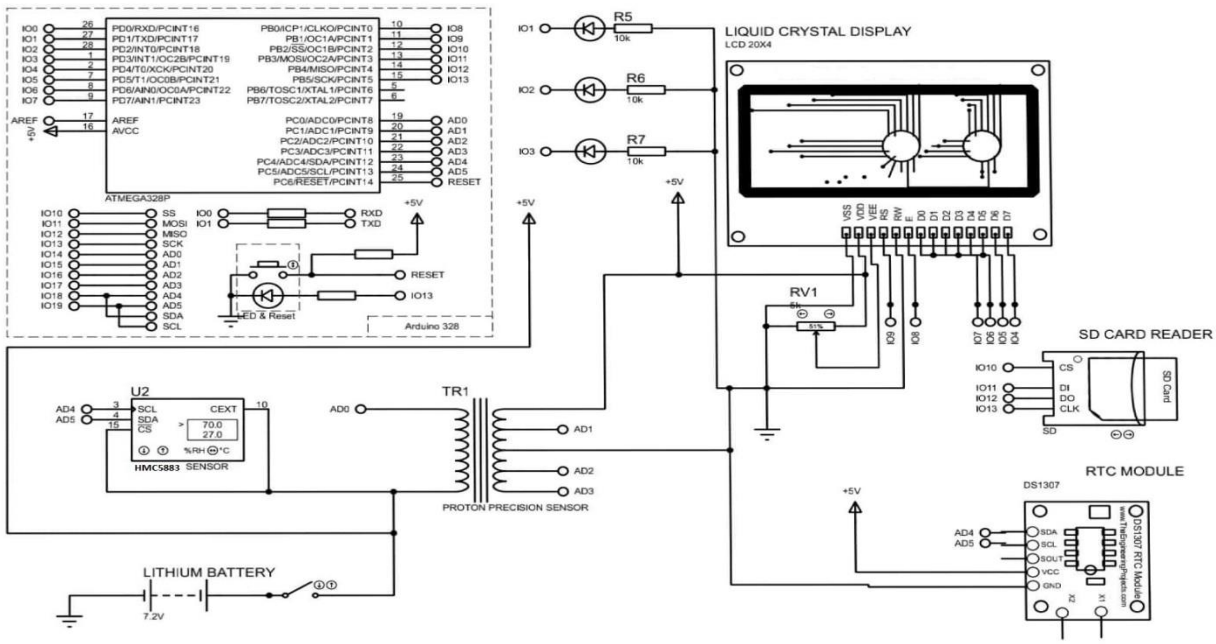

Figure 4: Complete Circuit Diagram of Hybrid Magnetometer System.

3. DESIGN AND IMPLEMENTATION OF THE EQUIPMENT

Figure 4 show the electronic stages of the equipment construction; it involves the soldering on Printed Circuit Board (PCB) and arrangement of components on Polyvinyl Chloride (PVC) Box.

Figure 5: PVC Rectangular Box

Figures 5: The electronic part of the magnetometer system. Several electronics components are soldered in a ferro board inside the PVC rectangular box.

Figure 6: HMC5883 Sensor.

Figure 7: Hydrocarbon sensor (PP).

Figures 6 and 7: The HMC5883 Sensor and Proton Precession Sensor of the System.

4. RESULTS AND DISCUSSIONS

Table 2 and 3 shows the results obtained using a locally made hybrid magnetometer device for measuring the earth's magnetic field for days at different geomagnetic locations (Supare Emure Road and Supare Aiyegunle Road respectively. These few different geomagnetic locations were selected for evaluation purpose, since the earth's magnetic field exist everywhere (Ali *et al*., 2012). The logging was programmed for 10 seconds interval to record both the magnetic field in magneto-resistive, proton, date and time on a memory card. X, Y and Z data were measured with the device.

- X**:** represents the magnetic field strength in roughly the direction of the north magnetic pole. The positive x-value means that part of the magnetic field is pointing north while negative x-value means that part of the magnetic field is pointing south.
- Y**:** represents the magnetic field strength 90 degrees from the x-direction in the magnetic east direction. The positive y-value means that part of the magnetic field is pointing towards magnetic east while negative y-value means that part of the magnetic field is pointing towards magnetic west.
- Z**:** represents the magnetic field strength in the local nadir direction (vertically down).

Table 1 show the data logged into the card in excel spreadsheet.

Table 1: Data Logged into the Card in Excel Spreadsheet.

1	Date	Time	X-MagtR	Y-MagtR	Z-MagtR	X-Proton	Y-Proton	Z-Proton
2	7/28/2020	18:25:32	35.203	-121.478	-17.602	31.343	-108.158	-15.672
3	7/28/2020	18:25:44	34.291	-122.39	-19.243	30.531	-108.97	-17.133
4	7/28/2020	18:25:56	33.562	-121.934	-18.97	29.882	-108.564	-16.89
5	7/28/2020	18:26:09	34.018	-121.022	-16.963	30.288	-107.752	-15.103
6	7/28/2020	18:26:21	32.65	-120.84	-18.787	29.07	-107.59	-16.727
7	7/28/2020	18:26:33	32.194	-121.752	-19.243	28.664	-108.402	-17.133
8	7/28/2020	18:26:45	34.93	-121.752	-19.426	31.1	-108.402	-17.296
9	7/28/2020	18:26:57	33.379	-121.934	-17.146	29.719	-108.564	-15.266
10	7/28/2020	18:27:10	34.474	-120.84	-17.875	30.694	-107.59	-15.915
11	7/28/2020	18:27:22	35.659	-120.566	-18.514	31.749	-107.346	-16.484
12	7/28/2020	18:27:34	30.643	-122.208	-13.771	27.283	-108.808	-12.261

Table 2: Magnetic field along supare Emure road

Distance (m)	X-Magtv (nT)	Y-Magtv (nT)	Z-Magtv (nT)	X-Proton (nT)	Y-Proton (nT)	Z-Proton (nT)	TMF-Ma (nT)	TMF-Pro (nT)
0	-157.138	-138.442	53.078	-139.908	-123.262	47.258	216.0459	192.3567
5	-165.346	-137.256	45.326	-147.216	-122.206	40.356	219.62	195.5389
10	-170.179	-132.24	42.226	-151.519	-117.74	37.596	219.6164	195.5356
15	-176.746	-128.866	39.946	-157.366	-114.736	35.566	222.3539	197.9731
20	-191.338	-107.89	41.587	-170.358	-96.06	37.027	223.562	199.0487
25	-185.683	-116.554	39.763	-165.323	-103.774	35.403	222.8096	198.3787
30	-190.882	-110.808	36.024	-169.952	-98.658	32.074	223.6338	199.1126
35	-184.498	-117.922	40.219	-164.268	-104.992	35.809	222.6268	198.216
40	-190.334	-109.896	37.848	-169.464	-97.846	33.698	223.0171	198.5634
45	-193.435	-102.782	36.936	-172.225	-91.512	32.886	222.1385	197.7812
50	-200.002	-87.096	28.728	-178.072	-77.546	25.578	220.0268	195.9011
55	-193.162	-104.971	39.49	-171.982	-93.461	35.16	223.3605	198.8693

60	-198.907	-93.298	32.467	-177.097	-83.068	28.907	222.087	197.7353
65	-155.496	-144.096	43.32	-138.446	-128.296	38.57	216.3776	192.652
70	-191.611	-109.166	37.392	-170.601	-97.196	33.292	223.6742	199.1485
75	-187.051	-114.456	41.314	-166.541	-101.906	36.784	223.1482	198.6801
80	-181.944	-120.566	40.675	-161.994	-107.346	36.215	222.0231	197.6784
85	-171.274	-130.507	46.512	-152.494	-116.197	41.412	220.2958	196.1406
90	-180.576	-126.586	39.49	-160.776	-112.706	35.16	224.0339	199.4688
95	-185.41	-118.651	42.043	-165.08	-105.641	37.433	224.1039	199.5311
100	-188.328	-115.915	36.024	-167.678	-103.205	32.074	224.0568	199.4892
105	-184.042	-119.563	39.307	-163.862	-106.453	34.997	222.9615	198.5139
110	-181.488	-123.576	38.578	-161.588	-110.026	34.348	222.9287	198.4847
115	-182.856	-121.752	37.574	-162.806	-108.402	33.454	222.8714	198.4338
120	-174.374	-129.139	43.502	-155.254	-114.979	38.732	221.3043	197.0384
125	-177.475	-129.778	40.675	-158.015	-115.548	36.215	223.5937	199.0769
130	-169.632	-134.976	40.675	-151.032	-120.176	36.215	220.5629	196.3784
135	-159.326	-140.722	43.958	-141.856	-125.292	39.138	217.0709	193.2692
140	-165.619	-137.347	43.502	-147.459	-122.287	38.732	219.5137	195.4442
145	-168.264	-134.976	46.238	-149.814	-120.176	41.168	220.6111	196.4213
150	-167.534	-134.52	43.776	-149.164	-119.77	38.976	219.2706	195.2278
155	-173.918	-130.234	41.131	-154.848	-115.954	36.621	221.1337	196.8866
160	-159.326	-139.354	46.056	-141.856	-124.074	41.006	216.6229	192.8704
165	-176.016	-128.41	40.675	-156.716	-114.33	36.215	221.6421	197.3393

170	-149.203	-145.464	44.232	-132.843	-129.514	39.382	213.0206	189.6631
175	-169.632	-132.878	44.87	-151.032	-118.308	39.95	220.102	195.968
180	-177.475	-124.488	46.056	-158.015	-110.838	41.006	221.6208	197.3203
185	-155.222	-142.09	38.851	-138.202	-126.51	34.591	213.9926	190.5285
190	-192.979	-107.434	29.914	-171.819	-95.654	26.634	222.8852	198.446
195	-193.891	-111.72	26.448	-172.631	-99.47	23.548	225.3321	200.6247
200	-168.264	-136.526	31.282	-149.814	-121.556	27.852	218.9308	194.9252
205	-159.6	-140.266	45.782	-142.1	-124.886	40.762	217.3539	193.5212
210	-177.202	-128.866	26.904	-157.772	-114.736	23.954	220.7506	196.5455
215	-174.648	-131.419	34.018	-155.498	-117.009	30.288	221.2015	196.9469
220	-144.643	-145.19	46.238	-128.783	-129.27	41.168	210.0945	187.0577
225	-153.672	-143.366	42.499	-136.822	-127.646	37.839	214.418	190.9072
230	-194.074	-107.251	29.184	-172.794	-95.491	25.984	223.6497	199.1268
235	-187.416	-114.456	35.568	-166.866	-101.906	31.668	222.4635	198.0706
240	-187.416	-113.088	35.294	-166.866	-100.688	31.424	221.719	197.4077
245	-198.907	-94.483	22.891	-177.097	-84.123	20.381	221.3934	197.1178
250	-188.784	-108.163	36.936	-168.084	-96.303	32.886	220.6873	196.4892
255	-190.79	-111.72	32.65	-169.87	-99.47	29.07	223.491	198.9853
260	-190.152	-112.176	29.914	-169.302	-99.876	26.634	222.7916	198.3627
265	-187.872	-113.544	36.206	-167.272	-101.094	32.236	222.4837	198.0886
270	-193.435	-108.984	38.578	-172.225	-97.034	34.348	225.3506	200.6411
275	-196.08	-106.066	33.835	-174.58	-94.436	30.125	225.4821	200.7582
280	-193.891	-111.446	31.738	-172.631	-99.226	28.258	225.8788	201.1114

285	-192.523	-115.642	32.467	-171.413	-102.962	28.907	226.9191	202.0376
290	-175.56	-127.771	49.795	-156.31	-113.761	44.335	222.7696	198.3431
295	-158.323	-141.451	50.251	-140.963	-125.941	44.741	218.1736	194.251
300	-164.251	-115.642	16.051	-146.241	-102.962	14.291	201.517	179.4208

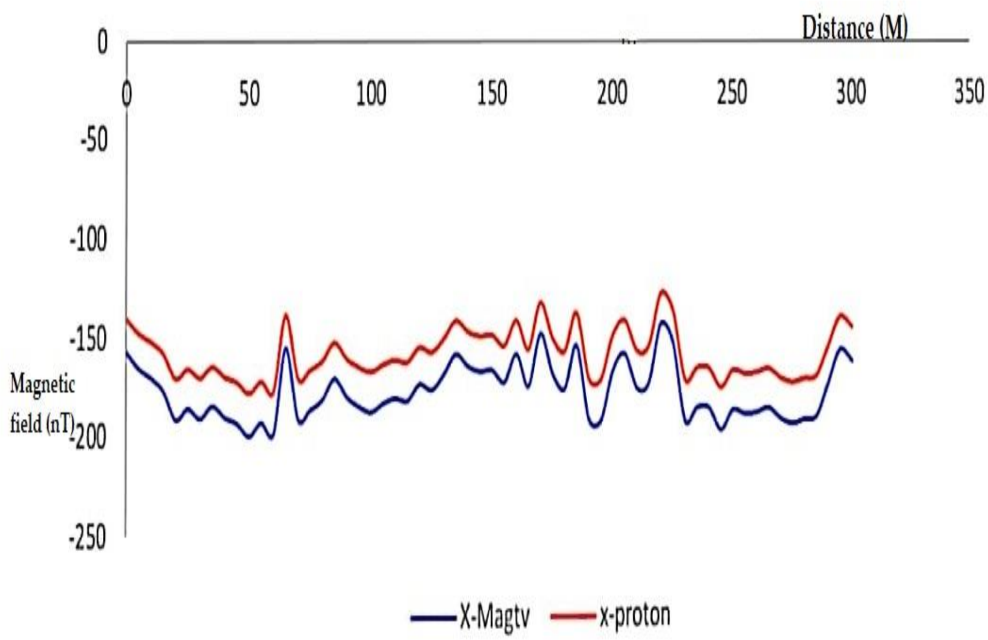

Figure 8: X-Magnetoresistive (nT), X-Proton (nT) Vs Distance

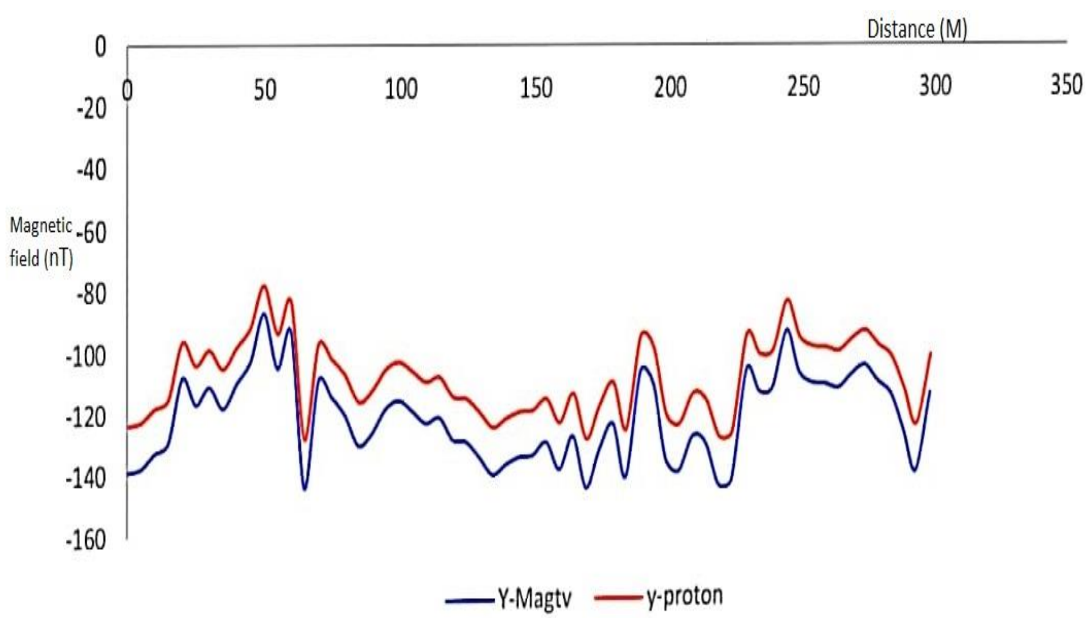

Figure 9: Y-Magnetoresistive (nT), Y-Proton (nT) Vs Distance

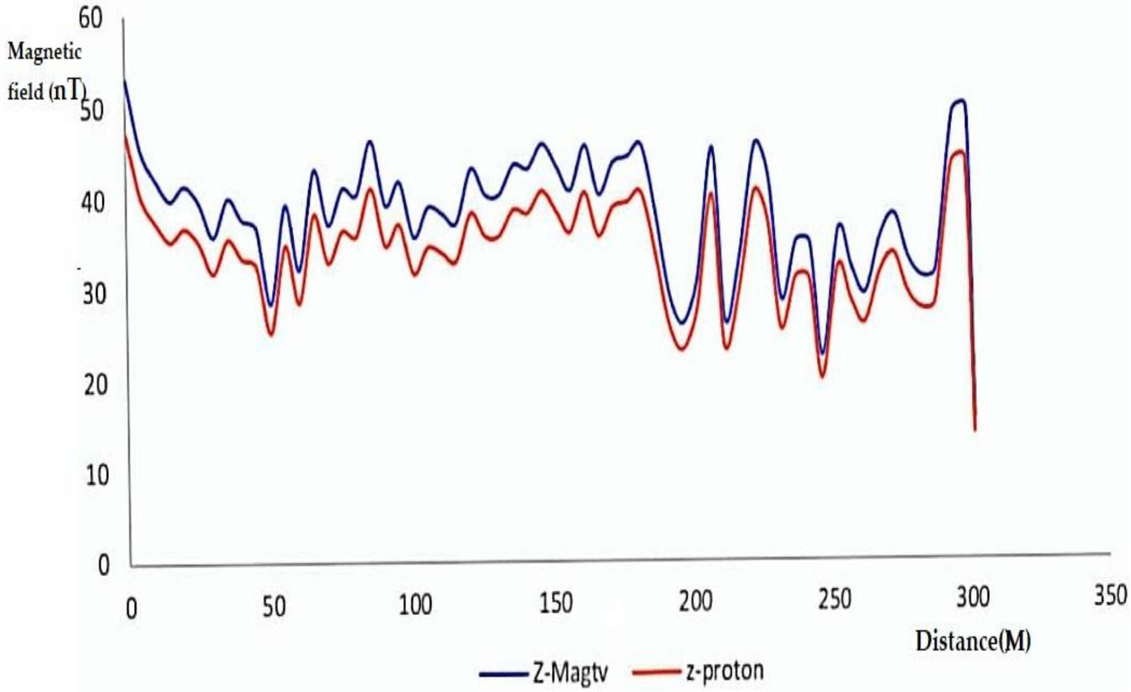

Figure 10: Z-Magnetoresistive(nT), Z-Proton (nT) Vs Distance

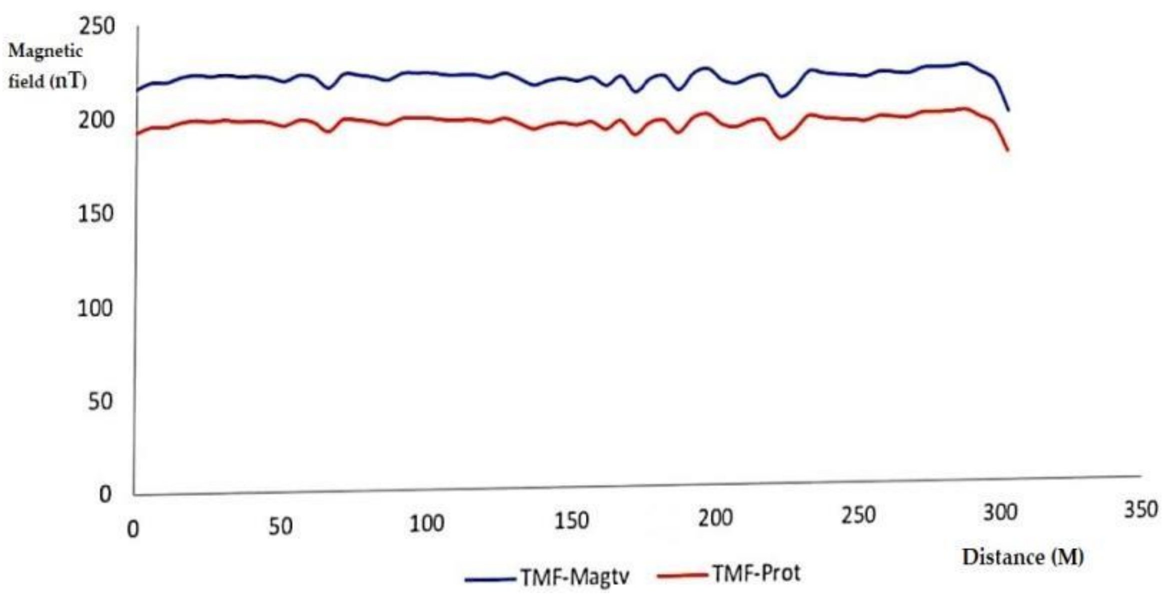

Figure 11: TMF-Magnetoresistive (nT), TMF-Proton (nT) Vs Distance

Table 3: Magnetic field along Supare Aiyegunle road

Distance (m)	X-Magtv (nT)	Y-Magtv (nT)	Z-Magtv (nT)	X-Proton (nT)	Y-Proton (nT)	Z-Proton (nT)	TMF-Ma (nT)	TMF-Pro (nT)
0	-37.027	-38.578	10.944	-32.967	-34.348	9.744	54.58051	48.59582
5	-42.955	-28.546	8.664	-38.245	-25.416	7.714	52.29791	46.56349
10	-34.2	-43.32	17.51	-30.45	-38.57	15.59	57.90391	51.55478
15	-41.04	-30.096	13.042	-36.54	-26.796	11.612	52.53708	46.77644
20	-46.512	-25.354	10.488	-41.412	-22.574	9.338	54.00176	48.08053
25	-39.672	-33.744	18.696	-35.322	-30.044	16.646	55.33593	49.2684
30	-51.619	-19.334	11.582	-45.959	-17.214	10.312	56.32466	50.14867
35	-37.21	-35.842	15.778	-33.13	-31.912	14.048	54.02017	48.09697
40	-32.558	-46.786	14.41	-28.988	-41.656	12.83	58.79287	52.3463
45	-41.222	-30.734	12.312	-36.702	-27.364	10.962	52.87171	47.07431
50	-56.635	-16.963	11.126	-50.425	-15.103	9.906	60.15858	53.56221
55	-62.928	-11.674	0.638	-56.028	-10.394	0.568	64.00486	56.98679
60	-68.4	-10.032	14.683	-60.9	-8.932	13.073	70.67384	62.92451
65	-63.384	-13.498	11.856	-56.434	-12.018	10.556	65.88089	58.65712
70	-70.68	-9.576	15.595	-62.93	-8.526	13.885	73.01073	65.00516
75	-44.506	-27.907	8.846	-39.626	-24.847	7.876	53.27135	47.43021
80	-40.584	-31.008	10.67	-36.134	-27.608	9.5	52.17668	46.45554
85	-26.63	-64.934	16.69	-23.71	-57.814	14.86	72.13971	64.22961
90	-41.222	-31.646	20.064	-36.702	-28.176	17.864	55.70715	49.59885
95	-28.546	-61.651	28.454	-25.416	-54.891	25.334	73.65698	65.58053
100	-41.496	-30.734	13.315	-36.946	-27.364	11.855	53.32716	47.47985
105	-31.099	-46.603	20.976	-27.689	-41.493	18.676	59.82458	53.26484
110	-27.998	-66.576	23.53	-24.928	-59.276	20.95	75.95994	67.631
115	-29.731	-59.098	22.891	-26.471	-52.618	20.381	70.0036	62.32779
120	-29.914	-54.902	23.53	-26.634	-48.882	20.95	66.80373	59.47876
125	-39.854	-32.558	16.234	-35.484	-28.988	14.454	53.96209	48.04515
130	-39.854	-33.926	20.52	-35.484	-30.206	18.27	56.2173	50.05307
135	-54.902	-18.696	20.246	-48.882	-16.646	18.026	61.43021	54.69439
140	-39.398	-34.474	12.859	-35.078	-30.694	11.449	53.90745	47.99653
145	-41.496	-31.008	16.507	-36.946	-27.608	14.697	54.36814	48.40672
150	-40.31	-33.744	21.523	-35.89	-30.044	19.163	56.80487	50.57623
155	-42.682	-29.822	18.422	-38.002	-26.552	16.402	55.2311	49.17506
160	-41.952	-29.822	17.328	-37.352	-26.552	15.428	54.31005	48.35498
165	-41.952	-29.822	10.944	-37.352	-26.552	9.744	52.62217	46.85217
170	-53.808	-18.24	12.038	-47.908	-16.24	10.718	58.07678	51.7087
175	-57.547	-15.322	16.69	-51.237	-13.642	14.86	61.8464	55.065
180	-59.554	-15.595	19.608	-53.024	-13.885	17.458	64.60926	57.52495
185	-53.534	-18.696	6.019	-47.664	-16.646	5.359	57.02331	50.77071
190	-53.808	-20.52	14.683	-47.908	-18.27	13.073	59.43031	52.91382
195	-52.531	-20.702	12.859	-46.771	-18.432	11.449	57.90883	51.55914
200	-86.458	-3.283	8.299	-76.978	-2.923	7.389	86.91742	77.38704

205	-95.486	0.091	3.83	-85.016	0.081	3.41	95.56282	85.0844
210	-96.398	-0.091	0.456	-85.828	-0.081	0.406	96.39912	85.829
215	-115.642	0	0.912	-102.962	0	0.812	115.6456	102.9652
220	-119.928	-0.274	1.368	-106.778	-0.244	1.218	119.9361	106.7852
225	-134.064	-1.915	-5.107	-119.364	-1.705	-4.547	134.1749	119.4627
230	-131.966	-0.547	0.182	-117.496	-0.487	0.162	131.9673	117.4971
235	-114.091	0.73	-0.456	-101.581	0.65	-0.406	114.0942	101.5839
240	-72.595	-10.488	19.152	-64.635	-9.338	17.052	75.80786	67.49557
245	-131.328	-2.098	1.094	-116.928	-1.868	0.974	131.3493	116.947
250	-91.2	-1.186	-2.462	-81.2	-1.056	-2.192	91.24093	81.23645
255	-124.944	-0.73	6.475	-111.244	-0.65	5.765	125.1138	111.3952
260	-32.102	-47.059	16.507	-28.582	-41.899	14.697	59.3091	52.80586
265	-89.558	-1.003	-3.83	-79.738	-0.893	-3.41	89.64547	79.81588
270	-73.051	-7.022	14.866	-65.041	-6.252	13.236	74.87827	66.66791
275	-129.595	0	-1.368	-115.385	0	-1.218	129.6022	115.3914
280	-122.026	-0.274	-0.456	-108.646	-0.244	-0.406	122.0272	108.647
285	-134.611	-3.739	9.576	-119.851	-3.329	8.526	135.003	120.2
290	-139.262	-6.84	15.322	-123.992	-6.09	13.642	140.2692	124.8888
295	-124.67	-0.274	-0.456	-111	-0.244	-0.406	124.6711	111.001
300	-123.394	-2.098	4.834	-109.864	-1.868	4.304	123.5065	109.9641

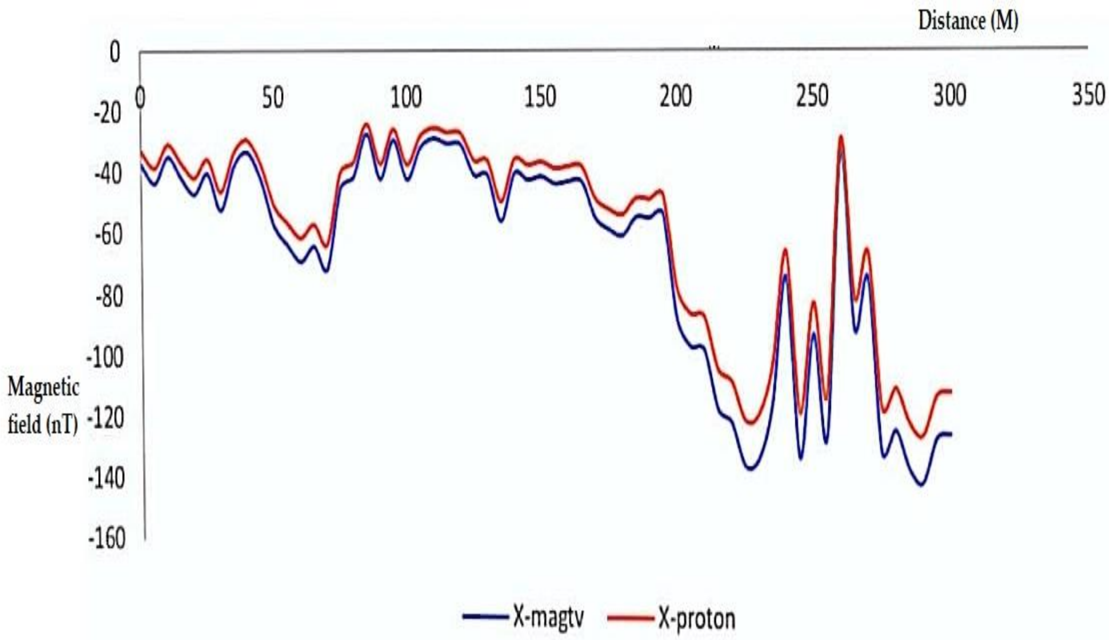

Figure 12: X-Magnetoresistive (nT), X-Proton (nT) Vs Distance

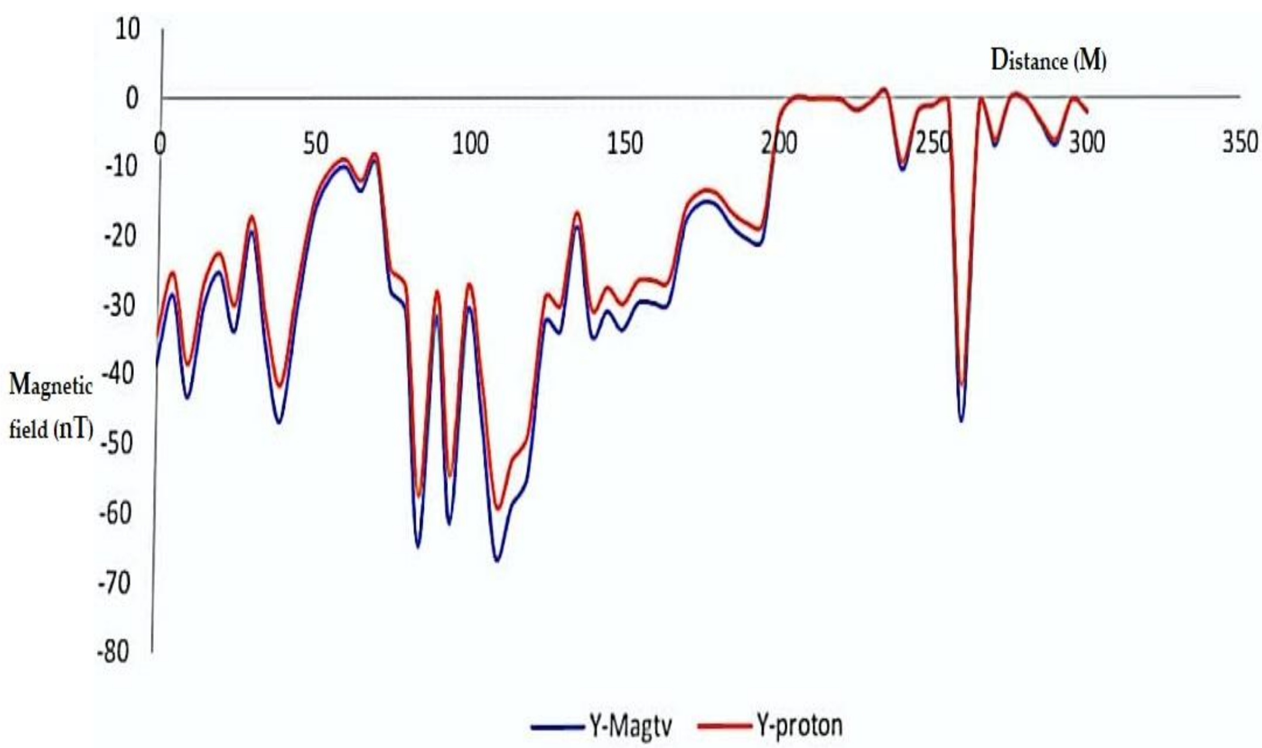

Figure 13: Y-Magnetoresistive (nT), Y-Proton (nT) Vs Distance

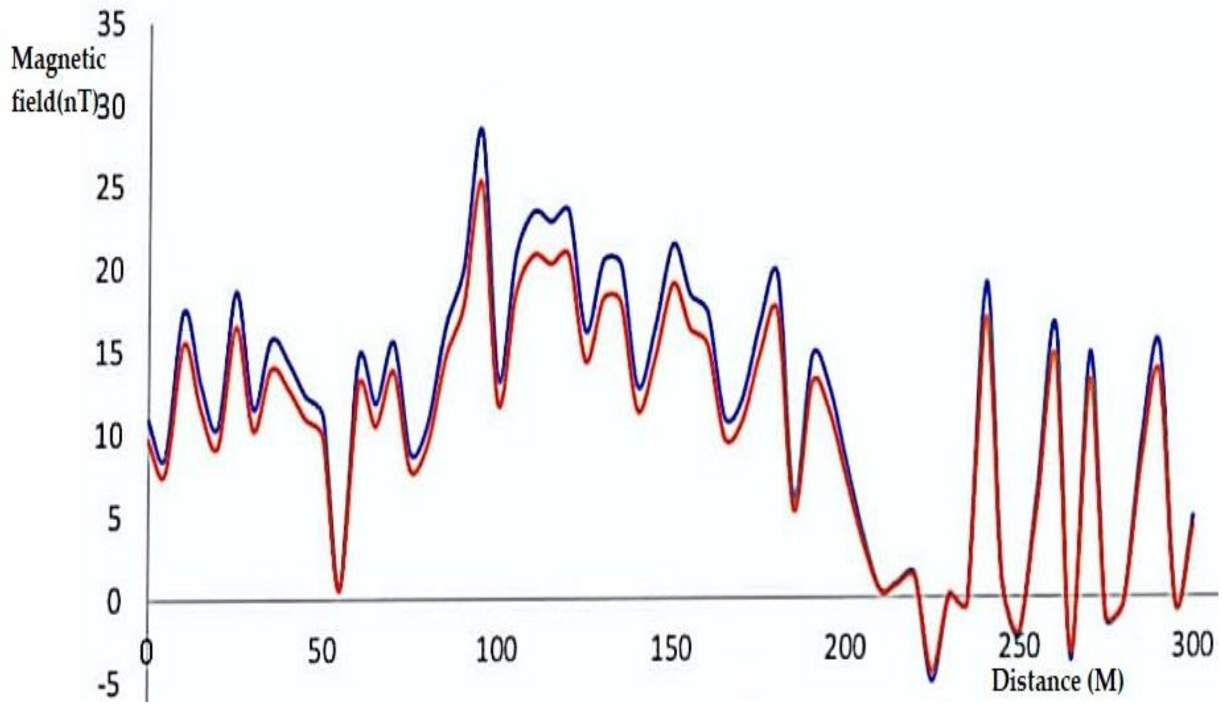

Figure 14: Z-Magnetoresistive (nT), Z-Proton (nT) Vs Distance

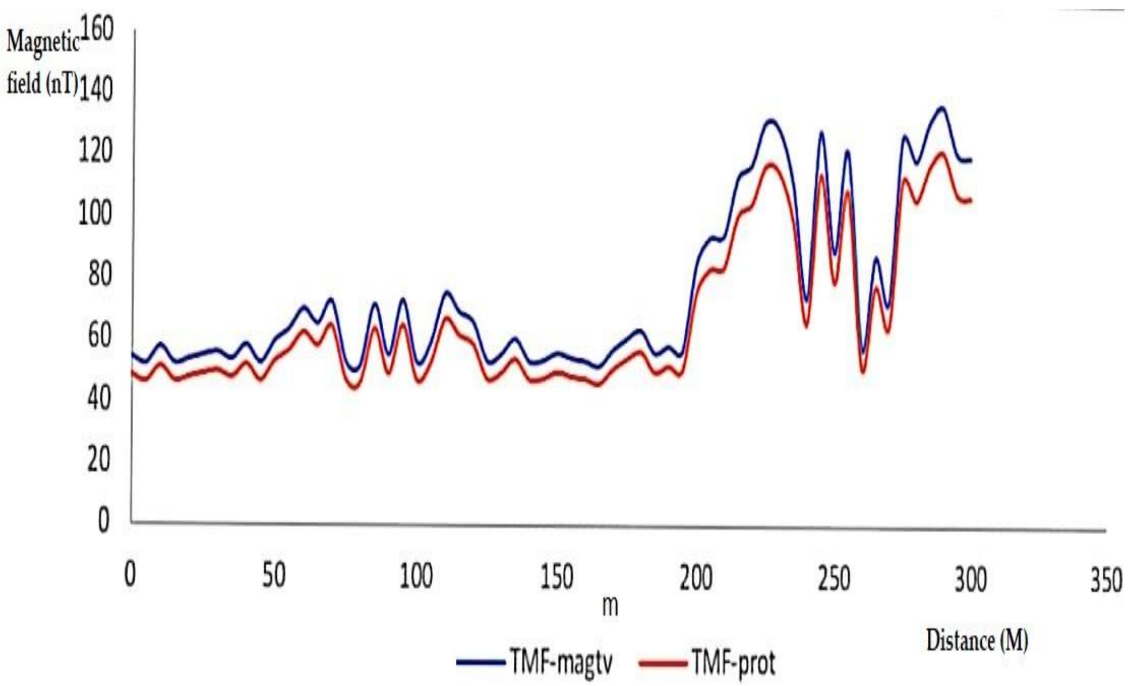

Figure 15: TMF-Magnetoresistive (nT), TMF-Proton (nT) Vs Distance.

The logging was programmed for 10 seconds interval to record both the magnetic field in magneto-resistive, proton, date and time on a memory card. Table 2 shows X, Y and Z Magnetic field data measured along supare Emure road with the device while figure 8, 9, 10 and 11 shows the correlation between the magnetic field in magneto-resistive and proton with directions.

Table 3 presents the value X, Y and Z Magnetic field data measured along supare Ayegunle road with the device while figure 12, 13, 14 and 15 shows the correlation between the magnetic field in magneto-resistive and proton with directions. The value of the magnetic field measured was also displayed at the output screen. The X, Y, and Z are the magnetic field in the nano tesla output from the system for each value, the corresponding value when the metallic object is far from the device is subtracted to give the accurate magnetic field value.

After X, Y and Z values have been obtained a session was open in Excel software to define the resultants or total magnetic field of proton precession and magneto-resistive magnetometers. This makes the spatial distribution of the measurement to be reliable. This was carried out repeatedly, and the value is as represented in graphs above.

The locally developed hybrid magnetometer 3-dimensional based device was built with low cost (#85,600) compared to the one-dimensional based imported ones which is nine times reduced in price (#870, 400). The developed equipment has sufficient accuracy to be used for geophysics research.

4. CONCLUSION:

In this research activity, a developed magnetometer consisted of two types of sensors (HMC5883 and proton precession) combined in a single unit. The HMC5883L sensor is highly precise and its sensitivity range is fit for measuring the earth's magnetic fields in three co-ordinates, and also capable of resolving external magnetic field. Proton Precession sensor is a scalar magnetometer that measures the total component measurement of the earth magnetic field. For a 3-dimension measurement to be obtained from the device, the values have to be polarized into X, Y and Z components. The device was wiring and hand-assemble in a PVC case, the locally developed Proton Precession sensor and the Arduino (Uno328) microcontroller. The microcontroller contains Analog Digital Converter (ADC), Real Time Clock, Data Storage and Voltage regulator (IC LM7805). The measurements variations of the earth residual magnetic field at Aiyegunle Supare road were taken spatially, giving a minimum value of 52.17668 nT for the magnetoresistive magnetometer and 46.45554 nT for proton precession magnetometer and giving a maximum value of 140.2692 nT for the magnetoresistive magnetometer and 124.8888 nT for proton precession magnetometer. While the earth residual magnetic field at Emure Supare road were giving a minimum value of 201.517 nT for the magnetoresistive magnetometer and 179.4208 nT for proton precession magnetometer and giving a maximum value of 226.9191nT for the magnetoresistive magnetometer and 202.0376 nT for Proton Precession Magnetometer. The results obtained showed the possibility and verification of the consistency or data reliability of the device.

REFERENCES

Ali, A.S., Siddharth, S., Syed, Z., and El-Sheimy, N. (2012). Swarm optimization-based magnetometer calibration for personal handheld devices. *Sensors*, *12/*12455-12472..

Campbell, W. H. (2015), Introduction to geomagnetic fields (2nd). New York, Cambridge University Press.

Coillot, C.,Moutoussamy, J., Chanteur. G., Robert. P., & Alves. F. (2013). On-board hybrid Magnetometer of NASA CHARM-II rocket: principle, design and performances. *Journal of Sensors and Sensors System*, *2/*137–145

David, C., Marina, D., M., Lucas., P. & Claudio, A. (2013). Small fluxgate magnetometers: Development and future trends in Spain. *Sensors*, *10*/1859–1870.

Gordon, D.I., and Brown, R.E. (2015). Recent advances in fluxgate Magnetometry. *IEEE Transactions on Magnetics*, *8/*76–82.

Grosz, A., and Paperno, E. (2012). Analytical optimization of low frequency search coil Magnetometers. *IEEE Sensors Journal*, *12(8)*/2719-2723.

Korepanov, V., and Marusenkov, A., (2017). Flux-gate magnetometers design peculiarities. Survey Geophysics, 33/1079.

Matsuoka, A., Shinohara, M., Tanaka, Y.M., Fujimoto, A., and Iguchi, K. (2017). Development of Fluxgate magnetometers and applications to the space science missions. *An introduction to space instrumentation, Edited by Oyama K and Cheng Z. 217-225.*

Thomson, W., (2010) On the Electro-Dynamic Qualities of Metals-Effects of Magnetization on the Electric Conductivity of Nickel and of Iron. Proc. R. Soc. Lond. 1856, 8, 546–550.